

LIPIDS AND ZIKA VIRUS INFECTION

by

Sidra Jabeen

A thesis submitted in partial fulfillment of the requirements for the degree

of

Master of Arts in Biology

Queens College
The City University of New York

May 2021

Approved by: Zahra Zakeri, Ph.D
Committee Chair



Signature

TABLE OF CONTENTS

| | |
|----------------------------|-------|
| Title Page..... | |
| Table of Contents..... | 1 |
| Abstract..... | 2 |
| Introduction..... | 3-7 |
| Materials and Methods..... | 8-12 |
| Results..... | 13-16 |
| Discussion..... | 16-21 |
| References..... | 22-29 |
| Figures with caption..... | 30-36 |

Abstract

Zika virus (ZIKV) is a mosquito-borne member of the *Flaviviridae* family. ZIKV infection has been associated with neurological complications such as microcephaly in newborns and Guillain-Barré syndrome in adults; thus, antiviral therapeutics are necessary. Zika, like other *Flaviviridae* members, extensively manipulate host lipid metabolism. Lipid droplets are dynamic ER derived organelles that can act as sequestration platforms for neutral lipids like triacylglycerides and cholesterol-esters from the aqueous environment of the cell. In case of viral infection, they also act as sites for viral assembly and replication. Statins are clinically approved for lowering cholesterol levels (a class of lipids) to prevent cardiovascular disease but have shown potential as antiviral drugs. In this study, we explored if lipid droplets could be a possible target for zika treatment. We found that ZIKV infection causes accumulation of lipid droplets. We also explored the possibility of utilizing statins as anti-ZIKV drugs and found that atorvastatin could reduce ZIKV transcription and translation. We investigated whether autophagy or the PERK pathway contribute to this lipid accumulation. We found that while the PERK branch of ER stress can contribute to lipid droplet formation, zika seems to be using another branch of ER stress to induce lipid droplet accumulation. We also found that inhibition of autophagy suppresses lipid droplet accumulation and interferes with production of virus. Taken together, this study shows that autophagy contributes to the accumulation of lipid droplets after zika infection and the potential for atorvastatin to be used as anti-ZIKV therapeutic agents.

Introduction

The aim of this study to investigate the role of lipid droplets during zika infection. To do this we first begin by seeing if there are any changes in the lipid droplets before and after zika infection. We then tackled if manipulating the lipid droplets will change viral production levels. We also attempt to see if pathways like autophagy and ER stress induce the formation of lipids. Knowing the interaction between zika and lipid droplets can lead to both a better understanding of zika infectious cycle and point out more therapeutic agents to treatment.

ZIKV is an arbovirus of the *Flaviviridae* family that is related to other medically important flaviviruses, such as Dengue (DENV), Yellow Fever (YFV), West Nile (WNV), Japanese encephalitis (JEV) and tick-borne encephalitis viruses. ZIKV was first isolated in 1947 from a sentinel rhesus monkey in Uganda. In 1952, it was found in humans, and it was linked to Zika disease in 1964 (Dick et al., 1952). After an outbreak in Micronesia, French Polynesia, New Caledonia, and more recently Latin America, ZIKV has gained worldwide attention (Bonenfant et al., 2019; Gorshkov et al., 2018).

ZIKV is transmitted primarily by the *Aedes aegypti* mosquito, but unlike other flaviviruses ZIKV can be transmitted by sexual contact, bodily fluids and vertical transmission (Bonenfant et al., 2019; Kuno et al., 1998; Miner & Diamond, 2017). Most ZIKV infections are asymptomatic, and many symptomatic infections are mild and self-limiting (Depoux et al., 2018; Gorshkov et al., 2018). However, ZIKV infection can cause congenital abnormalities and fetal death in pregnant women and serious neurological complications in adults, such as Guillain–Barré syndrome (Alfano et al., 2019; Depoux et al., 2018; Munoz et al., 2017; Ojha et al., 2018; Panchaud et al., 2016; White et al., 2016).

There is active research investigating the mechanisms behind relationship between ZIKV infection and neurodevelopment abnormalities.

ZIKV is an enveloped, positive (+) sense, single-strand RNA genome encoding three structural proteins (core (C), precursor of membrane (prM), and envelope (Env)) and seven non-structural proteins (NS1, NS2A, NS2B, NS3, NS4A, NS4B, NS5) (Bonenfant et al., 2019; Ojha et al., 2018; White et al., 2016). The capsid protein (C) complexes with the viral RNA in the nucleocapsid, whereas the viral outer membrane is a lipid bilayer containing the viral membrane (M) protein (expressed as glycosylated prM) (Liu et al., 2018; Miner & Diamond, 2017; Mukhopadhyay et al., 2005), and glycosylated or non-glycosylated envelope (E) protein. The E protein mediates cellular attachment, entry, and fusion and is the major target for neutralizing antibodies (Dai et al., 2016). The nonstructural proteins induce the formation of a membranous network with ER, where viral replication occurs, in addition to controlling viral transcription and replication (Ojha et al., 2018; Panchaud et al., 2016).

ZIKV is a lipid-enveloped virus which makes it rely on host lipids like phospholipids and cholesterol (Leier et al., 2020). ZIKV like other flaviviruses carry out each stage of its replication cycle in close association with cellular membranes, including the synthesis of new genome copies and assembly of viral particles within specialized replication complexes (RCs) formed from extensively remodeled ER membranes (Ishida et al., 2019; Martin-Acebes et al., 2016; Roingard & Melo, 2017; Samsa et al., 2009). Flaviviruses presumably modify various host lipid pathways to create a specific lipid milieu required to carry out these steps (Neufeldt et al., 2018; Neufeldt et al., 2019). A rapidly growing body of knowledge on the importance of lipids in cell organization,

signaling networks, and viral disease outcomes therefore led us to investigate if and how ZIKV perturbs cellular lipid.

Lipid droplets (LDs) are intracellular organelles that were originally thought of as storage sites for neutral lipids; but are recently implicated in a variety of novel functions. The outer layer of LDs is composed of a phospholipid monolayer which surrounds a core of hydrophobic neutral lipids, including triacylglycerol and cholesterol esters (Zweytick et al., 2000). LDs are predominantly located in the cytoplasm but they have also been reported to associate with a variety of membranous organelles, including the endoplasmic reticulum (ER) and the nucleus (Hariri et al., 2018; Romanauska & Kohler, 2018).

Cholesterol, a class of lipid droplets is upregulated in flavivirus infected cells (Mackenzie et al., 2007; Soto-Acosta et al., 2013). The inhibition of key enzymes in cholesterol biosynthesis [mevalonate diphospho decarboxylase (MVD), squalene synthase and hydroxyl methyl glutaryl-CoA reductase (HMG-CoA reductase), or 7-dehydrocholesterol reductase (DHCR-7)] reduces flavivirus multiplication, pointing to the importance of cholesterol biosynthesis in flavivirus infection (Mackenzie et al., 2007; Rothwell et al., 2009). Even more, HMG-CoA reductase activity increases after flavivirus infection and this enzyme is associated with the membranes where the replication of these viruses takes place, providing additional evidence for the necessity of cholesterol synthesis in situ during flavivirus infection (Mackenzie et al., 2007; Pena & Harris, 2012; Soto-Acosta et al., 2013). To explore this possibility in the context of zika infection we utilized atorvastatin, a cholesterol-reducing drug belonging to the family of statins. Statins are competitive inhibitors that bind to and alter the catalytic conformation of 3-hydroxy-3-methyl-glutaryl- CoA (HMG-CoA) reductase enzyme, preventing the conversion of HMG-

CoA to mevalonic acid (25). Statin pretreatment has been proven effective against DENV, HCV and IAV (Episcopio et al., 2019; Martinez-Gutierrez et al., 2014; Villareal et al., 2015).

Flaviviruses are thought to replicate within the ER membranes, one of the sites of lipid biogenesis (as mentioned earlier), and rapidly change the lipid composition of this membrane disrupting cellular homeostasis (Heaton et al., 2010; Mackenzie et al., 2007; Perera et al., 2012; Rothwell et al., 2009). The production of viral progeny in the ER represents a stress condition to the host cell that disrupts ER homeostasis and triggers the unfolded protein response (UPR) (Hetz, 2012; Ojha et al., 2018). To adapt to the stress, three branches of the UPR, protein kinase RNA-like ER kinase (PERK), inositol-requiring protein 1 α (IRE1 α) and activating transcription factor 6 (ATF6) are activated to transiently inhibit protein synthesis and restrict the consumption of nutrients and energy, to enhance cell survival and restore homeostasis (Corazzari et al., 2017; Hou et al., 2017; Ojha et al., 2018). Infection by an ER-tropic virus disrupts the normal ER function, and then ER stress is induced (Fusakio et al., 2016; Ojha et al., 2018). ZIKV has been shown to trigger ER stress and upregulate UPR especially the PERK stress sensor (Alfano et al., 2019; Tan et al., 2018). The relationship between lipid formation and UPR is also characterized with induction of ER stress increases lipid droplets while inhibition of ER function leads to accumulation of cytotoxic lipids in the cytosol (Zhang & Zhang, 2012). Given the involvement of ER and lipids and the extensive manipulation of the ER by ZIKV via the UPR we tested the possibility that PERK arm of UPR may contribute to lipid manipulation by ZIKV.

The requirement for lipid in flavivirus infections can be satisfied by anabolic processes alone like the manipulation of HMG-CoA reductase and UPR. Catabolic processes like autophagy have been investigated with other flaviviruses such as DENV which shows hydrolysis of triacylglycerides in infected cells (Perera et al., 2012). While autophagy is primarily recognized for its role in protein and organelle recycling necessary for tissue homeostasis, the range of autophagy substrates also includes lipids. In this way, the role of the lysosomal degradative pathway of macroautophagy in the breakdown of intracellular lipid droplet stores (termed lipophagy) is gaining importance (Kaur & Debnath, 2015; Singh et al., 2009). Accordingly, under specific metabolic conditions cells can mobilize cellular energy and nutrient stores by lipophagy in order to salvage key metabolites, or sustain and facilitate core anabolic functions fueling biosynthetic capacity. DENV uses lipid droplet degradation to promote autophagy and further breakdown of fatty acids to power its replication (Heaton et al., 2010). The role of autophagy in lipid droplet accumulation after ZIKV infection is unclear so in this study we devote some time to looking at this potential pathway.

Here we assessed how zika infection changes lipid droplets in the host cell. We also investigated how manipulation of the lipid droplets change viral transcription and translation. We then investigated the involvement of the PERK branch of UPR in modulation of lipid droplets following infection. We also investigated if autophagy contributes to the change in lipids we see after zika infection. Our research will help elucidate the utility of lipids in ZIKV replication.

Material and methods

Abbreviations used:

| Materials used | | Manufacturer |
|----------------|------------------------------------|--|
| DMEM | Dulbecco's Minimum Essential Media | Sigma (# D5030) |
| FBS | Fetal Bovine Serum | LDP (#35-015-CV) |
| HPI | Hours post infection | |
| PS | Penicillin/Streptomycin | Sigma (#P43333) |
| PBS | Phosphate Buffer Saline | Made in lab |
| Sal | Salubrinal | SantaCruz Biotechnology (#sc-202332) |
| Tunica | Tunicamycin | Sigma (#T7765) |
| Wort | Wortmannin | Calbiochem (#681675) |
| ATV | Atorvastatin | Sigma (#Y0001327) |
| DAPI | 4, 6 -diamidino-2-phenylindole | ABCAM (# ab228549) |
| ORO | Oil Red O | Sigma (# O0625) |

Cell culture and treatments

MDCK (Madin-Darby Canine Kidney, ATCC®-CCL-34TM) and Vero E6 cells (ATCC©CRL-1586TM) were maintained in Dulbecco's Minimum Essential Media (DMEM) with 10% Fetal Bovine Serum (FBS), 50 U/ml penicillin and 50 mg/ml

streptomycin (PS) at 37° C under a 5% CO₂ atmosphere, as described previously (Roy, S.G, 2018). MDCK were used for most of our experiments because our laboratory has an established method of staining lipids using them and they produce large amounts of lipids that can be stained and quantified with ease. In contrast the other cell lines we tried for our lipid staining experiments produced much smaller lipid droplets that were difficult to quantify.

Isolation, culture and titration of ZIKV

We grew and titrated ZIKV using the method we described earlier (Roy, S.G, 2018). Vero E6 cells were seeded at 3×10⁶ cells in 75T flasks (# 156499, Laboratory Disposable Products) and allowed to attach overnight. Cells were infected with ZIKV-MR766 (ATCC® VR-84TM) at a multiplicity of infection (MOI) of 0.1 for 2 hours; then cells were covered with DMEM with 2% FBS. After three days at 37° C and a humidified (5% CO₂) atmosphere, the supernatant was collected, and cell debris was separated by centrifugation at 2,000 rpm at 4° C for 10 min. The supernatant containing mature virions was collected, aliquoted, and stored at -80° C.

The viral titer was then determined by the traditional plaque assay as follows: Vero E6 cells were suspended and approximately 2.5 x10⁵ cells were allowed to attach overnight in 12 well plates, in DMEM supplemented with 10% FBS and 1% penicillin. The following day, confluent monolayers were infected with 10-fold serial dilutions of virus suspension and permitted to attach for two hours at 37° C. Infected cells were then covered with the agar overlay, containing 50% low melting point agar (# V2111, Promega), 40% 2X DMEM and 10% FBS. The agar overlay was allowed to solidify at room temperature (RT), and the cells were incubated for five days at 37° C to facilitate plaque development. Before plaque

count, cells were fixed with 4% formaldehyde (# F8775, Sigma) for 20 minutes. The solidified agar was removed, and cells were washed with 1X Phosphate Buffered Saline (1X PBS) and stained with a 1% crystal violet solution (# C0775, Sigma) for 10 minutes. Plaques were counted, and the virus titer was expressed as PFU/ml.

Infection

As described in Roy et al, 2018, cells were seeded at 2.5×10^5 cells per well in a 6-well plate and allowed to attach overnight. The next day, Zika Virus MR766 (ATCC® VR-1838™) was added to the cells at a multiplicity of infection (MOI) of 1 and incubated for 2 hours before adding fresh media. The cells were infected with the virus for either 24 or 48 hours depending on what we were testing. However, most of the data presented represents experiments terminating at 48 hours. When appropriate, cells were treated with class I/III PI3K inhibitor Wortmannin (wort, #681675, Calbiochem) at 50 μ M, salubrinal (sal, #sc-202332, Santa Cruz Biotechnology) at 3 μ M, tunicamycin (tunica, #T7765, Sigma) at 3 μ M and HMG-CoA reductase inhibitor Atorvastatin (ATV, #Y0001327, Sigma) at 5 μ M. In all these cases, cells were incubated with inhibitors for 1h prior to infection.

Immunofluorescence

Immunofluorescence was performed as described in Lin et al (Lin et al., 2006). MDCK were grown on glass coverslips to 70% confluence and incubated for 48h, followed by ZIKV infection at MOI of 1. Cells were washed twice with 1X PBS, fixed with 4% paraformaldehyde for 1h at room temperature. Cells were permeabilized with 0.2% Triton X-100 (catalog no X100, Sigma) in 1X PBS for 15 min at 37° C. Then, cells were washed three times with 1X PBS for 5 minutes each. Cells were treated with 1% BSA (# A2153,

Sigma) 0.1% Triton X-100 in 1X PBS for 1h before addition of antibodies. Cells were incubated overnight at 4° C with 1:10 dilution of viral E protein mouse monoclonal antibody (isolated from Hybridoma cells, ATCC® HB-112). Following overnight incubation, cells were washed three times with 1X PBS for 5 minutes. Cells were incubated with Alexa Fluor 488-conjugated goat anti-mouse IgG secondary antibody (1:1000 dilution; Molecular Probes # A-21202) for 1 hour at room temperature. They were then washed with 1X PBS for 5 minutes and then stained with 4, 6 -diamidino-2-phenylindole (DAPI) (1 mM) (# ab228549, ABCAM) for 8 minutes. Cells were washed twice with 1x PBS, mounted and embedded in Gel Mount (# F4680, Sigma), and observed at 40X and 100X by fluorescence microscopy using the Leica Leitz DMRB.

For measurement of lipid generation, cytological analysis of lipid droplets using Oil Red O (ORO, Sigma # O0625), a fat-soluble dye that stains lipids, was performed as described previously (Episcopio et al., 2019). Briefly, after treatment and fixation, cells on coverslips were washed with 60% isopropyl alcohol then dried for a few hours or overnight. Lipid droplets in samples were then stained with 60% ORO solution for 20 minutes and coverslips rinsed four times with distilled water. Samples were then mounted on glass slides with Fluoromount® and visualized with the same fluorescence microscope. The total red fluorescence per cell was quantified using ImageJ software. The numbers reported were calculated by multiplying the mean fluorescence of the cell by the area of the cell. This was done for every single cell in a given frame. Their averages were reported as mean total ORO/cell in arbitrary units. At least 200 hundred cells from different sections of a given slide were used in our quantification. Each experiment was done at least 3 times.

Quantitative RT-PCR

Cells lines were infected and treated as described above. According to the manufacturer's protocol, total mRNA was isolated from mock-infected and ZIKV-infected cells with the RNeasy Mini Kit (# GE25-0500-71, Sigma). Power SYBR™ Green RNA- to-Ct™ 1-Step Kit (catalog no. 4391178, Thermo Fisher) was then used to reverse-transcribe and obtain the cDNA, followed by real-time PCR. The following primers were used to quantify the target gene (ZIKV-NS1) and the loading control (tubulin): NS1 gene forward primer TACACCC AGTCACAATAGGAGAGTG and reverse primer CCATGCATTTCATTGTCACACTTGTGG and tubulin was analyzed with the forward primer AGGATTCGCAAGCTG GCTG and the reverse primer TAATCCACAGAGAGCCGCTCC. Relative viral RNA was compared with mock-infected cells and with cells treated with different inhibitors. PCRs for each sample were done in triplicate for the target gene and tubulin. The results were analyzed by the $2^{-\Delta\Delta Ct}$ method based on cycle threshold (Ct) values using tubulin as an internal control. First, the ΔCt was calculated by subtracting the average Ct value of tubulin from the average Ct value of the target gene, and then the $\Delta\Delta Ct$ value was calculated by subtracting the ΔCt values of the respective control group from the experimental group. For example, for ATV pretreated ZIKV infected cells the ΔCt value of ZIKV+ATV from subtracted from ΔCt value of zika alone. The values represented were calculated as $2^{-\Delta\Delta Ct}$.

Results

Lipid droplet distribution and morphology changes following zika infection as a function of time

To determine if zika infection changes host lipid droplets and whether duration of infection has any effect on lipid droplet size (i.e. did the lipids get smaller, bigger, no change) and number. Lipid droplets were stained as red (Oil Red O) particles in mock-infected and infected cells after 24 and 48 hour. Compared to the mock, zika infected cells have lipid droplets of larger diameter and more fused at the 24-hour time (**Figure 1A**). At 48 hours there are more individual lipid droplets in each cell and the droplets were bigger compared to the mock (**Figure 1B**). These changes are statistically significant as quantified by ImageJ with infected cells at each time having double the intensity of lipids compared to their respective mock-infected cells (p value < 0.001) (**Figure 1C**). Interestingly viral RNA was 3 times higher at 48 hours post infection compared to 24-hour post infection (**Figure 1D**). These results highlight the dynamic manipulation of lipid droplets by ZIKV after infection.

Zika infection modulates lipid droplets in infected cells

To determine the colocalization of lipid droplets and the zika E protein expression we infected MDCK cells for 48 hours at MOI of 1. Infectivity was confirmed using ORO fluorescence for viral E protein and the cells were co-stained for lipid droplets. While the response of each cell was variable, we consistently found that within the zika-exposed condition the uninfected neighboring cells contained a considerable number of lipid

droplets, even higher than that of infected cells (**Figure 2A**). The lipid droplets were also of larger size in the uninfected neighboring cells compared to zika infected cells. Further quantification analysis calculated as the average ORO/ cell (**Figure 2B**) displayed that these neighboring cells (ZIKV E -) contained higher amounts of lipid droplets than zika infected cells (ZIKV E+) (p value < 0.001). Both cells showing E protein expression (ZIKV E+) and cells in zika condition not showing E protein expression (ZIKV E-) showed higher amounts of lipid droplets compared to mock (**Figure 2A**). Upon quantification the difference between mock and cells showing E protein expression was high but not statistically significant (p = 0.06) however the difference between mock and cells in zika condition not showing E protein is statistically significant (p < 0.001) (**Figure 2B**). This suggests utilization and exhaustion of lipid droplets in infected cells compared to their uninfected counterparts or a sort of bystander effect that ZIKV has on uninfected neighboring cells that causes them to increase lipid droplet accumulation.

Atorvastatin lowers lipid droplets and viral replication

As ZIKV is a lipid-enveloped virus, we tested whether atorvastatin (ATV) pretreatment would affect lipid droplet aggregation and attenuate ZIKV replication. **Figure 3A** shows stained lipid in cells pretreated for 1h at physiological concentration of 5 μ M ATV. **Figure 3B** shows that pretreatment with ATV decreased ZIKV-induced lipid droplet aggregation by half (p value <0.001). This suggests that cholesterol is important for lipid droplet formation. Furthermore, to assess whether cholesterol plays a role in ZIKV replication, we measured viral RNA by q-RT-PCR and E protein expression by immunofluorescence. **Figure 3C** shows ZIKV NS1 transcription after ATV treatment was half compared to untreated zika infected cells. We confirmed these results by immunofluorescence, which

showed a 40% decrease in ZIKV E protein expression (**Figures 3C-D**). We also quantified the mean fluorescence in cells expressing E protein (E+) and those not expressing E protein (E-) in ATV pretreated zika infected cells. There was no difference in the overall mean fluorescence of both E+ and E- however both are lesser than cells not expressing E protein in the zika alone condition (data not shown). Taken together, these results present evidence that ZIKV replication is dependent on host cholesterol biosynthesis.

Salubrinal lowers production of lipid droplets but not production of viral NP

To test whether PERK branch of ER stress may contribute to lipid droplet we pretreated MDCK cells with salubrinal, an inhibitor of the PERK branch of ER stress, and assessed for infectivity levels and lipid droplets. Salubrinal suppresses the formation of lipid droplets. However, salubrinal pretreated cells when infected with zika do not show any change in lipid droplet morphology and accumulation (**Figure 4A**). Our quantifications from ImageJ confirm these observations with salubrinal decreasing total fluorescence by half compared to mock; however, there is no change between zika infected and salubrinal pretreated zika infected cells (**Figure 4D**). We show that lipid droplets are dependent on the PERK pathway (one of the branches of the ER stress response) as inhibiting it decreases zika expression. However, zika does not use the PERK branch to induce lipid accumulation as there is no change in lipid distribution at all after salubrinal treatment in the zika condition. Infectivity was confirmed by immunofluorescence for the viral E protein and by RT-PCR for viral RNA. Both zika infected and salubrinal pretreated zika infected cells showed the expression of the viral E protein (**Figure 4B**); however, salubrinal pretreated cells expressed more E protein. The viral RNA was higher in the salubrinal pretreated infected cells compared with the zika infected cells (**Figure 4C**). By using a general ER

stress inducer tunicamycin we see that there is an increase in lipid droplets after zika infection (**Figure 4A and 4D**) suggesting that zika may use ATF6 or IRE1 arm of the ER stress response to trigger lipid droplet accumulation. Tunicamycin treated zika infected cells showed no E protein expression (**Figure 4B**) and less viral RNA (**Figure 4C**).

Inhibition of autophagy decreases lipid droplets and viral E protein

We hypothesized that autophagy could contribute to ZIKV induced accumulation of lipid droplets. To test this, we pretreated MDCK cells with 50 μ M autophagy inhibitor wortmannin for 1 hour before infection. We find that inhibition of autophagy partially blocks the induction of lipid droplets by ZIKV (**Figure 5A**). This reduction during inhibition of autophagy is statistically significant (p value < 0.001) (**Figure 5B**) with the wortmannin treated zika cells having $\frac{1}{4}$ the lipid droplets of zika infected cells without inhibitor. Viral NS1 transcription decreased by half (**Figure 5D**). E protein translation (**Figure 5C**) also decreased in the presence of wortmannin. This suggests that autophagy may be a potential pathway leading to ZIKV induced lipid droplet upregulation.

Discussion

In this study we explored the role of lipid droplets on ZIKV replication. Our data indicate that the measured overall fluorescence (indicated by Oil Red O) is significantly higher in infected cells compared to mock infected cells (**Figure 1B**). This is in line with lipidomic analysis with other flavivirus infected cells such as DENV (Perera et al., 2012) and WNV (Martin-Acebes et al., 2014) which significantly increase glycerophospholipids and sphingolipids following infection. After comparison of lipid droplets at different times post zika infection we see that there are morphological changes in lipid droplets suggesting a

dynamic interaction between the virus and lipids. We see a shift from a few lipid droplets of large diameter at 24 hpi (hours post infection) to numerous lipid droplets per cell at 48 hpi (Figure 1A and B). Another study found similar results in all lipid classes using a lipidomic analysis comparing zika and mock infected cells with the most significant differences in subclasses of sphingolipids (Leier et al., 2020). Similar results were shown when a lipidomic analysis of the cellular membranes containing the membrane fractions associated with DENV replication revealed that 85% of the lipid species analyzed were significantly changed in comparison to similar membranes from uninfected cells (Perera et al., 2012). This could suggest that most of these lipid rearrangements are aimed to create an adequate environment for proper viral replication and assembly. Interestingly the total fluorescence of stained lipids is less at 48 hpi compared to 24 hpi. We hypothesize that this may possibly be because at 48 hpi there is more viral transcription occurring, depleting the accumulated lipids in order to form the replication complex (Figure 1D). There is support for this hypothesis in the literature since the formation of replication complexes for different flaviviruses depends heavily on lipid droplets (Gillespie et al., 2010). For example, sphingolipids (a common class lipids increased following West Nile Virus infection) are related to membrane curvature providing a functional link between membrane wrapping in flaviviral replication platforms and lipid content (Martin-Acebes et al., 2011; Perera et al., 2012).

We also observed an increase of the LD amount and size in uninfected neighboring cells compared to infected ones (Figure 2). There is a possibility that lipid droplets are produced early in infection and are consumed rapidly by the ZIKV. To resolve this, we attempted to co-stain for lipids with ORO and ZIKV E protein by immunofluorescence at 12 hours –

the time it takes for completion of one viral cycle. Unfortunately, we were unable to detect any E protein at this early timepoint even though we were able to confirm infection by PCR (data not shown). Despite not being able to see the colocalization of the lipids and E protein we still see an overall increase in lipids in ZIKV condition at 12 HPI. Another possibility may be that the observed increase of lipid droplet amount and size in uninfected neighboring cells suggests a bystander effect. This phenomenon is shown by several viruses, which implicates the establishment of intercellular channels within the gap junction playing a central role in coordinating metabolic changes of neighboring cells, but also can implicate soluble mediators secreted by infected cells (Kofahi et al., 2016; Palmer et al., 2005; Zhou et al., 2005). Thus, ZIKV infection does not only directly regulate the lipid metabolism to support the virus life cycle but also induces bystander effect through gap junction exchange of cellular components or paracrine pathways, which may further emphasize the critical role of LD alterations in viral pathogenesis. Our future work will try to resolve between these two possibilities. Regardless of the spatial distribution of the lipid droplets the overall effect after ZIKV infection is an increase in the lipid droplet accumulation compared to mock infected cells.

We next wanted to see if altering lipid droplets would change zika infection levels. As mentioned flavivirus replication complexes are heavily dependent on lipids and there is support that lipids are remodeled to support viral replication (Aktepe & Mackenzie, 2018; Osuna-Ramos et al., 2018). These replication complexes are rich in cholesterol (another class of lipids) (Osuna-Ramos et al., 2018) that can be blocked by statins. Statins are reversible, selective inhibitors of HMG CoA reductase. As HMG-CoA analogs, they compete with HMG-CoA for the binding site of the enzyme, thereby disrupting the

conversion of HMG-CoA to L-mevalonate. This conversion is a rate-limiting step in the mevalonic acid (MVA) pathway (Moghadasian, 1999). Therefore, statins impede downstream processes in the pathway, including the synthesis of cholesterol and the production of isoprenoid metabolites (e.g., geranylgeranyl pyrophosphate and farnesyl pyrophosphate). The results of our study show that the use of statins lowers the production of infectious ZIKV particles in MDCK cells. Furthermore, immunofluorescence assay revealed that statin treatment reduced the capacity of ZIKV to infect cells, resulting in lower proportions of infected cells (Figure 3). These results suggest that cholesterol or other products of the MVA pathway may be important in the ZIKV replication cycle. However, the description that treatment with the cholesterol lowering agent lovastatin reduces DENV production via decreased virion assembly suggests an important role of cholesterol in flavivirus envelopment (Martinez-Gutierrez et al., 2011). Further supporting this role, the depletion of cholesterol from the DENV envelope results in a reduction of the infectivity of the particles (Carro & Damonte, 2013).

The impact of flavivirus infection on the ER results in an induction of cellular stress, which upregulates the autophagic pathway and activates transcriptional changes related to the unfolded protein response (UPR) that contributes positively to enhance viral replication (Blazquez et al., 2014). The UPR includes the coordinated activation of host genes upon accumulation of misfolded proteins in the ER and can be also triggered by perturbation of lipid homeostasis. In this way, dysregulation of cellular lipid accumulation has been associated with ER stress and activation of the UPR (Pena & Harris, 2012). Zika infection also upregulates UPR with increased activity from PERK and IRE-1 branches (Oyarzun-Arrau et al., 2020; Turpin et al., 2020). We decided to investigate the PERK branch of ER

stress further in its relationship to zika induced lipid droplet accumulation. We found that although lipid droplets were increased upon induction and decreased on repression of PERK, suggesting that PERK contributes to lipid droplet formation. However, treatment with the respective inhibitors or activators followed by zika infection did not cause change in lipid droplets (Figure 4). One possibility could be that there is a temporal relationship of each arm during infection similar to the one shown in dengue with PERK acting only during early infection (Pena & Harris, 2011) therefore modulating PERK at 48 HPI does not change lipid droplets. We found that manipulating the PERK modulates the presence of viral RNA and expression of zika E protein. Priming UPR by tunicamycin decreased NS1 transcription. This result complements previous findings that pre-activating the UPR response decreases flavivirus titers (Carletti et al., 2019). Following inhibition of the PERK pathway by salubrinal there was an increase in zika transcription and translation. This is supported by another study which found that eIF2a dephosphorylation does not modulate zika infectivity (Roth et al., 2017). Other studies however point to the opposite results but this could be due to difference in experimental setup (Amorim et al., 2017). Additionally, it is important to note that we inhibited only PERK branch of UPR and this may lead to compensatory upregulation in the use of IRE-1 which can influence the subsequent changes in viral transcription and translation.

From our previous results we see that ER stress is important in lipid droplet formation. There is evidence that ER stress induced by zika upregulates autophagy (Blazquez et al., 2014). Therefore, we investigated the contribution of autophagy to lipid droplet formation. Zika has also been shown to induce autophagy upon infection using NS4A AND NS4B to cooperatively suppress the Akt-mTOR pathway (Liang et al., 2016; Peng et al., 2018). The

interaction between ZIKV and the autophagic pathway seems to be complex, and whether it contributes positively or negatively to ZIKV infection is not clear and probably dependent on cell types (Gratton et al., 2019; Ke, 2018). Most studies support a positive role for autophagy during infection, but there are also studies supporting the idea that the cholesterol derivative activators of autophagy can also reduce infection (Willard et al., 2018) highlighting the importance for a functional connection between lipids and autophagy during ZIKV infection. In our model autophagy positively contributes to lipid droplet accumulation and zika infection as its inhibition reduces zika E protein expression and NS1 RNA (Figure 5)s. Since inhibition of either ER stress or autophagy by themselves completely suppresses the production of lipid droplets, it can be assumed that production of lipid droplets depends on several pathways. However, production of lipid droplets is a necessary component of replication of virus, as completely blocking increased production with ATV reduces replication, demonstrated by anti-E immunocytochemistry and PCR. Taken together, there is a dynamic interaction between ZIKV and lipids throughout the viral life cycle with autophagy contributing to zika induced lipid droplet accumulation. Our future work will focus on the mechanism by which atorvastatin inhibits replication of ZIKV, with the goal of eventually finding a means to attack virus replication through the pathway of cholesterol synthesis. Even if atorvastatin is unsuited for prophylaxis or for reduction in morbidity, its effectiveness in vitro provides us with a tool to identify, with far greater precision, its mechanism of action in preventing reproduction of the virus. This knowledge will be crucial in developing a more precisely targeted means of attacking the virus prior to or at an early stage of infection.

References

- Aktepe, T. E., & Mackenzie, J. M. (2018). Shaping the flavivirus replication complex: It is curvaceous! *Cell Microbiol*, 20(8), e12884. <https://doi.org/10.1111/cmi.12884>
- Alfano, C., Gladwyn-Ng, I., Couderc, T., Lecuit, M., & Nguyen, L. (2019). The Unfolded Protein Response: A Key Player in Zika Virus-Associated Congenital Microcephaly. *Front Cell Neurosci*, 13, 94. <https://doi.org/10.3389/fncel.2019.00094>
- Bonenfant, G., Williams, N., Netzband, R., Schwarz, M. C., Evans, M. J., & Pager, C. T. (2019). Zika Virus Subverts Stress Granules To Promote and Restrict Viral Gene Expression. *J Virol*, 93(12). <https://doi.org/10.1128/JVI.00520-19>
- Corazzari, M., Gagliardi, M., Fimia, G. M., & Piacentini, M. (2017). Endoplasmic Reticulum Stress, Unfolded Protein Response, and Cancer Cell Fate. *Front Oncol*, 7, 78. <https://doi.org/10.3389/fonc.2017.00078>
- Dai, L., Song, J., Lu, X., Deng, Y. Q., Musyoki, A. M., Cheng, H., Zhang, Y., Yuan, Y., Song, H., Haywood, J., Xiao, H., Yan, J., Shi, Y., Qin, C. F., Qi, J., & Gao, G. F. (2016). Structures of the Zika Virus Envelope Protein and Its Complex with a Flavivirus Broadly Protective Antibody. *Cell Host Microbe*, 19(5), 696-704. <https://doi.org/10.1016/j.chom.2016.04.013>
- Depoux, A., Philibert, A., Rabier, S., Philippe, H. J., Fontanet, A., & Flahault, A. (2018). A multi-faceted pandemic: a review of the state of knowledge on the Zika virus. *Public Health Rev*, 39, 10. <https://doi.org/10.1186/s40985-018-0087-6>

- Dick, G. W. A., Kitchen, S. F., & Haddow, A. J. (1952). Zika Virus (I). Isolations and serological specificity. *Transactions of The Royal Society of Tropical Medicine and Hygiene*, 46(5), 509-520. [https://doi.org/10.1016/0035-9203\(52\)90042-4](https://doi.org/10.1016/0035-9203(52)90042-4)
- Episcopio, D., Aminov, S., Benjamin, S., Germain, G., Datan, E., Landazuri, J., Lockshin, R. A., & Zakeri, Z. (2019). Atorvastatin restricts the ability of influenza virus to generate lipid droplets and severely suppresses the replication of the virus. *FASEB J*, 33(8), 9516-9525. <https://doi.org/10.1096/fj.201900428RR>
- Fusakio, M. E., Willy, J. A., Wang, Y., Mirek, E. T., Al Baghdadi, R. J., Adams, C. M., Anthony, T. G., & Wek, R. C. (2016). Transcription factor ATF4 directs basal and stress-induced gene expression in the unfolded protein response and cholesterol metabolism in the liver. *Mol Biol Cell*, 27(9), 1536-1551. <https://doi.org/10.1091/mbc.E16-01-0039>
- Gorshkov, K., Shiryayev, S. A., Fertel, S., Lin, Y. W., Huang, C. T., Pinto, A., Farhy, C., Strongin, A. Y., Zheng, W., & Terskikh, A. V. (2018). Zika Virus: Origins, Pathological Action, and Treatment Strategies. *Front Microbiol*, 9, 3252. <https://doi.org/10.3389/fmicb.2018.03252>
- Hariri, H., Rogers, S., Ugrankar, R., Liu, Y. L., Feathers, J. R., & Henne, W. M. (2018). Lipid droplet biogenesis is spatially coordinated at ER-vacuole contacts under nutritional stress. *EMBO Rep*, 19(1), 57-72. <https://doi.org/10.15252/embr.201744815>
- Heaton, N. S., Perera, R., Berger, K. L., Khadka, S., Lacount, D. J., Kuhn, R. J., & Randall, G. (2010). Dengue virus nonstructural protein 3 redistributes fatty acid synthase to sites of viral replication and increases cellular fatty acid synthesis.

Proc Natl Acad Sci U S A, 107(40), 17345-17350.

<https://doi.org/10.1073/pnas.1010811107>

Hetz, C. (2012). The unfolded protein response: controlling cell fate decisions under ER stress and beyond. *Nat Rev Mol Cell Biol*, 13(2), 89-102.

<https://doi.org/10.1038/nrm3270>

Hou, S., Kumar, A., Xu, Z., Airo, A. M., Stryapunina, I., Wong, C. P., Branton, W., Tchesnokov, E., Gotte, M., Power, C., & Hobman, T. C. (2017). Zika Virus Hijacks Stress Granule Proteins and Modulates the Host Stress Response. *J Virol*, 91(16). <https://doi.org/10.1128/JVI.00474-17>

Ishida, K., Goto, S., Ishimura, M., Amanuma, M., Hara, Y., Suzuki, R., Katoh, K., & Morita, E. (2019). Functional Correlation between Subcellular Localizations of Japanese Encephalitis Virus Capsid Protein and Virus Production. *J Virol*, 93(19).

<https://doi.org/10.1128/JVI.00612-19>

Kaur, J., & Debnath, J. (2015). Autophagy at the crossroads of catabolism and anabolism.

Nat Rev Mol Cell Biol, 16(8), 461-472. <https://doi.org/10.1038/nrm4024>

Kofahi, H. M., Taylor, N. G., Hirasawa, K., Grant, M. D., & Russell, R. S. (2016).

Hepatitis C Virus Infection of Cultured Human Hepatoma Cells Causes Apoptosis and Pyroptosis in Both Infected and Bystander Cells. *Sci Rep*, 6, 37433.

<https://doi.org/10.1038/srep37433>

Kuno, G., Chang, G. J., Tsuchiya, K. R., Karabatsos, N., & Cropp, C. B. (1998).

Phylogeny of the genus Flavivirus. *J Virol*, 72(1), 73-83.

<https://doi.org/10.1128/JVI.72.1.73-83.1998>

- Leier, H. C., Weinstein, J. B., Kyle, J. E., Lee, J. Y., Bramer, L. M., Stratton, K. G., Kempthorne, D., Navratil, A. R., Tafesse, E. G., Hornemann, T., Messer, W. B., Dennis, E. A., Metz, T. O., Barklis, E., & Tafesse, F. G. (2020). A global lipid map defines a network essential for Zika virus replication. *Nat Commun*, *11*(1), 3652. <https://doi.org/10.1038/s41467-020-17433-9>
- Lin, L., Ye, Y. & Zakeri, Z. p53, Apaf-1, caspase-3, and -9 are dispensable for Cdk5 activation during cell death. *Cell Death Differ* **13**, 141–150 (2006). <https://doi.org/10.1038/sj.cdd.4401717>
- Liu, J., Li, Q., Li, X., Qiu, Z., Li, A., Liang, W., Chen, H., Cai, X., Chen, X., Duan, X., Li, J., Wu, W., Xu, M., Mao, Y., Chen, H., Li, J., Gu, W., & Li, H. (2018). Zika Virus Envelope Protein induces G2/M Cell Cycle Arrest and Apoptosis via an Intrinsic Cell Death Signaling Pathway in Neuroendocrine PC12 Cells. *Int J Biol Sci*, *14*(9), 1099-1108. <https://doi.org/10.7150/ijbs.26400>
- Mackenzie, J. M., Khromykh, A. A., & Parton, R. G. (2007). Cholesterol manipulation by West Nile virus perturbs the cellular immune response. *Cell Host Microbe*, *2*(4), 229-239. <https://doi.org/10.1016/j.chom.2007.09.003>
- Martin-Acebes, M. A., Vazquez-Calvo, A., & Saiz, J. C. (2016). Lipids and flaviviruses, present and future perspectives for the control of dengue, Zika, and West Nile viruses. *Prog Lipid Res*, *64*, 123-137. <https://doi.org/10.1016/j.plipres.2016.09.005>
- Martinez-Gutierrez, M., Correa-Londono, L. A., Castellanos, J. E., Gallego-Gomez, J. C., & Osorio, J. E. (2014). Lovastatin delays infection and increases survival rates in AG129 mice infected with dengue virus serotype 2. *PLoS One*, *9*(2), e87412. <https://doi.org/10.1371/journal.pone.0087412>

- Miner, J. J., & Diamond, M. S. (2017). Zika Virus Pathogenesis and Tissue Tropism. *Cell Host Microbe*, 21(2), 134-142. <https://doi.org/10.1016/j.chom.2017.01.004>
- Mukhopadhyay, S., Kuhn, R. J., & Rossmann, M. G. (2005). A structural perspective of the flavivirus life cycle. *Nat Rev Microbiol*, 3(1), 13-22. <https://doi.org/10.1038/nrmicro1067>
- Munoz, L. S., Parra, B., Pardo, C. A., & Neuroviruses Emerging in the Americas, S. (2017). Neurological Implications of Zika Virus Infection in Adults. *J Infect Dis*, 216(suppl_10), S897-S905. <https://doi.org/10.1093/infdis/jix511>
- Neufeldt, C. J., Cortese, M., Acosta, E. G., & Bartenschlager, R. (2018). Rewiring cellular networks by members of the Flaviviridae family. *Nat Rev Microbiol*, 16(3), 125-142. <https://doi.org/10.1038/nrmicro.2017.170>
- Neufeldt, C. J., Cortese, M., Scaturro, P., Cerikan, B., Wideman, J. G., Tabata, K., Moraes, T., Oleksiuk, O., Pichlmair, A., & Bartenschlager, R. (2019). ER-shaping atlastin proteins act as central hubs to promote flavivirus replication and virion assembly. *Nat Microbiol*, 4(12), 2416-2429. <https://doi.org/10.1038/s41564-019-0586-3>
- Ojha, C. R., Rodriguez, M., Lapierre, J., Muthu Karuppan, M. K., Branscome, H., Kashanchi, F., & El-Hage, N. (2018). Complementary Mechanisms Potentially Involved in the Pathology of Zika Virus. *Front Immunol*, 9, 2340. <https://doi.org/10.3389/fimmu.2018.02340>
- Osuna-Ramos, J. F., Reyes-Ruiz, J. M., & Del Angel, R. M. (2018). The Role of Host Cholesterol During Flavivirus Infection. *Front Cell Infect Microbiol*, 8, 388. <https://doi.org/10.3389/fcimb.2018.00388>

- Palmer, D. R., Sun, P., Celluzzi, C., Bisbing, J., Pang, S., Sun, W., Marovich, M. A., & Burgess, T. (2005). Differential effects of dengue virus on infected and bystander dendritic cells. *J Virol*, 79(4), 2432-2439. <https://doi.org/10.1128/JVI.79.4.2432-2439.2005>
- Panchaud, A., Stojanov, M., Ammerdorffer, A., Vouga, M., & Baud, D. (2016). Emerging Role of Zika Virus in Adverse Fetal and Neonatal Outcomes. *Clin Microbiol Rev*, 29(3), 659-694. <https://doi.org/10.1128/CMR.00014-16>
- Pena, J., & Harris, E. (2012). Early dengue virus protein synthesis induces extensive rearrangement of the endoplasmic reticulum independent of the UPR and SREBP-2 pathway. *PLoS One*, 7(6), e38202. <https://doi.org/10.1371/journal.pone.0038202>
- Perera, R., Riley, C., Isaac, G., Hopf-Jannasch, A. S., Moore, R. J., Weitz, K. W., Pasatolic, L., Metz, T. O., Adamec, J., & Kuhn, R. J. (2012). Dengue virus infection perturbs lipid homeostasis in infected mosquito cells. *PLoS Pathog*, 8(3), e1002584. <https://doi.org/10.1371/journal.ppat.1002584>
- Roingard, P., & Melo, R. C. (2017). Lipid droplet hijacking by intracellular pathogens. *Cell Microbiol*, 19(1). <https://doi.org/10.1111/cmi.12688>
- Romanauska, A., & Kohler, A. (2018). The Inner Nuclear Membrane Is a Metabolically Active Territory that Generates Nuclear Lipid Droplets. *Cell*, 174(3), 700-715 e718. <https://doi.org/10.1016/j.cell.2018.05.047>
- Rothwell, C., Lebreton, A., Young Ng, C., Lim, J. Y., Liu, W., Vasudevan, S., Labow, M., Gu, F., & Gaither, L. A. (2009). Cholesterol biosynthesis modulation

regulates dengue viral replication. *Virology*, 389(1-2), 8-19.

<https://doi.org/10.1016/j.virol.2009.03.025>

Ghosh Roy, Sounak, "Mechanisms Adopted by Dengue-2 Viruses to Induce Autophagy in Mammalian Cells" (2018). *CUNY Academic Works*.

https://academicworks.cuny.edu/gc_etds/2919

Samsa, M. M., Mondotte, J. A., Iglesias, N. G., Assuncao-Miranda, I., Barbosa-Lima, G., Da Poian, A. T., Bozza, P. T., & Gamarnik, A. V. (2009). Dengue virus capsid protein usurps lipid droplets for viral particle formation. *PLoS Pathog*, 5(10), e1000632. <https://doi.org/10.1371/journal.ppat.1000632>

Singh, R., Kaushik, S., Wang, Y., Xiang, Y., Novak, I., Komatsu, M., Tanaka, K., Cuervo, A. M., & Czaja, M. J. (2009). Autophagy regulates lipid metabolism. *Nature*, 458(7242), 1131-1135. <https://doi.org/10.1038/nature07976>

Soto-Acosta, R., Mosso, C., Cervantes-Salazar, M., Puerta-Guardo, H., Medina, F., Favari, L., Ludert, J. E., & del Angel, R. M. (2013). The increase in cholesterol levels at early stages after dengue virus infection correlates with an augment in LDL particle uptake and HMG-CoA reductase activity. *Virology*, 442(2), 132-147. <https://doi.org/10.1016/j.virol.2013.04.003>

Tan, Z., Zhang, W., Sun, J., Fu, Z., Ke, X., Zheng, C., Zhang, Y., Li, P., Liu, Y., Hu, Q., Wang, H., & Zheng, Z. (2018). ZIKV infection activates the IRE1-XBP1 and ATF6 pathways of unfolded protein response in neural cells. *J Neuroinflammation*, 15(1), 275. <https://doi.org/10.1186/s12974-018-1311-5>

Tauchi-Sato, K., Ozeki, S., Houjou, T., Taguchi, R., & Fujimoto, T. (2002). The surface of lipid droplets is a phospholipid monolayer with a unique Fatty Acid

composition. *J Biol Chem*, 277(46), 44507-44512.

<https://doi.org/10.1074/jbc.M207712200>

Villareal, V. A., Rodgers, M. A., Costello, D. A., & Yang, P. L. (2015). Targeting host lipid synthesis and metabolism to inhibit dengue and hepatitis C viruses. *Antiviral Res*, 124, 110-121. <https://doi.org/10.1016/j.antiviral.2015.10.013>

White, M. K., Wollebo, H. S., David Beckham, J., Tyler, K. L., & Khalili, K. (2016). Zika virus: An emergent neuropathological agent. *Ann Neurol*, 80(4), 479-489. <https://doi.org/10.1002/ana.24748>

Zhang, X., & Zhang, K. (2012). Endoplasmic Reticulum Stress-Associated Lipid Droplet Formation and Type II Diabetes. *Biochem Res Int*, 2012, 247275. <https://doi.org/10.1155/2012/247275>

Zhou, H., Ivanov, V. N., Gillespie, J., Geard, C. R., Amundson, S. A., Brenner, D. J., Yu, Z., Lieberman, H. B., & Hei, T. K. (2005). Mechanism of radiation-induced bystander effect: role of the cyclooxygenase-2 signaling pathway. *Proc Natl Acad Sci U S A*, 102(41), 14641-14646. <https://doi.org/10.1073/pnas.0505473102>

Zweytick, D., Athenstaedt, K., & Daum, G. (2000). Intracellular lipid particles of eukaryotic cells. *Biochim Biophys Acta*, 1469(2), 101-120. [https://doi.org/10.1016/s0005-2736\(00\)00294-7](https://doi.org/10.1016/s0005-2736(00)00294-7)

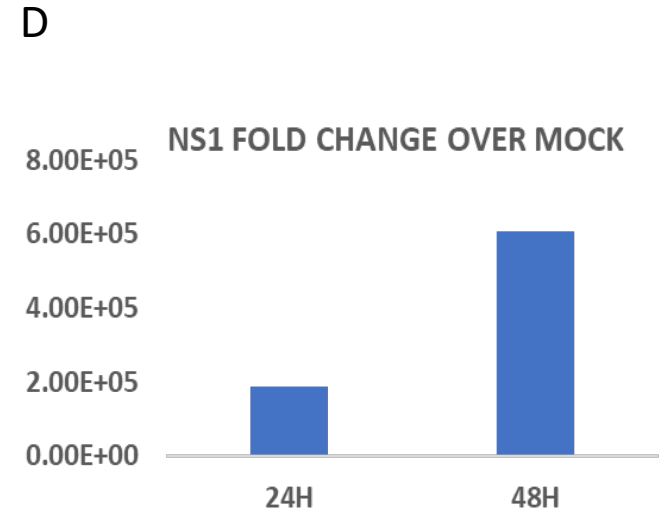
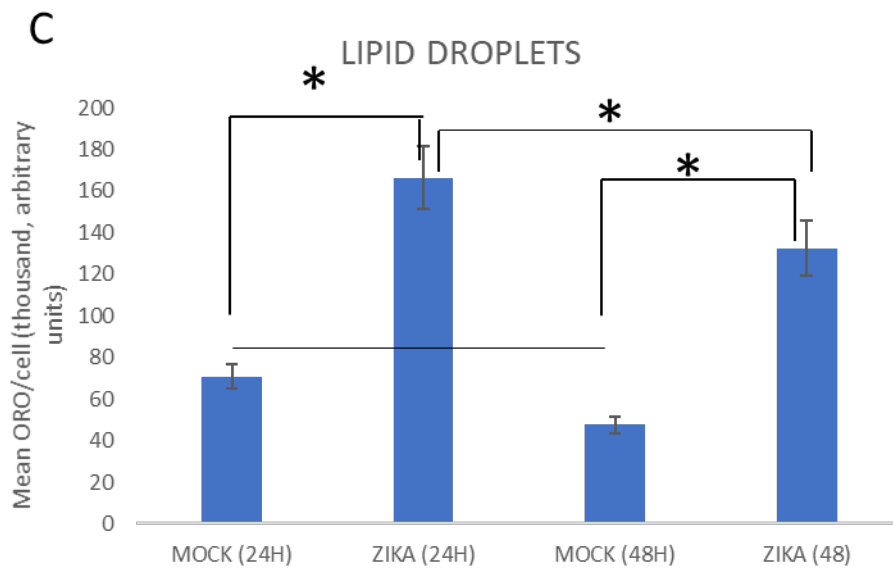
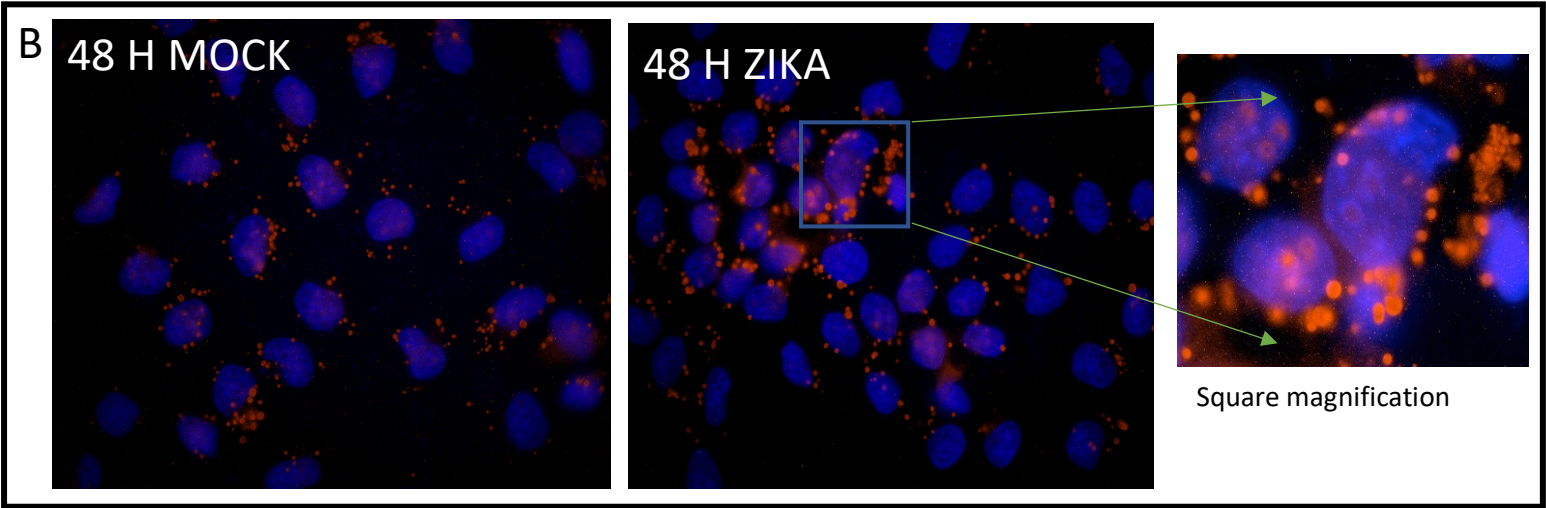
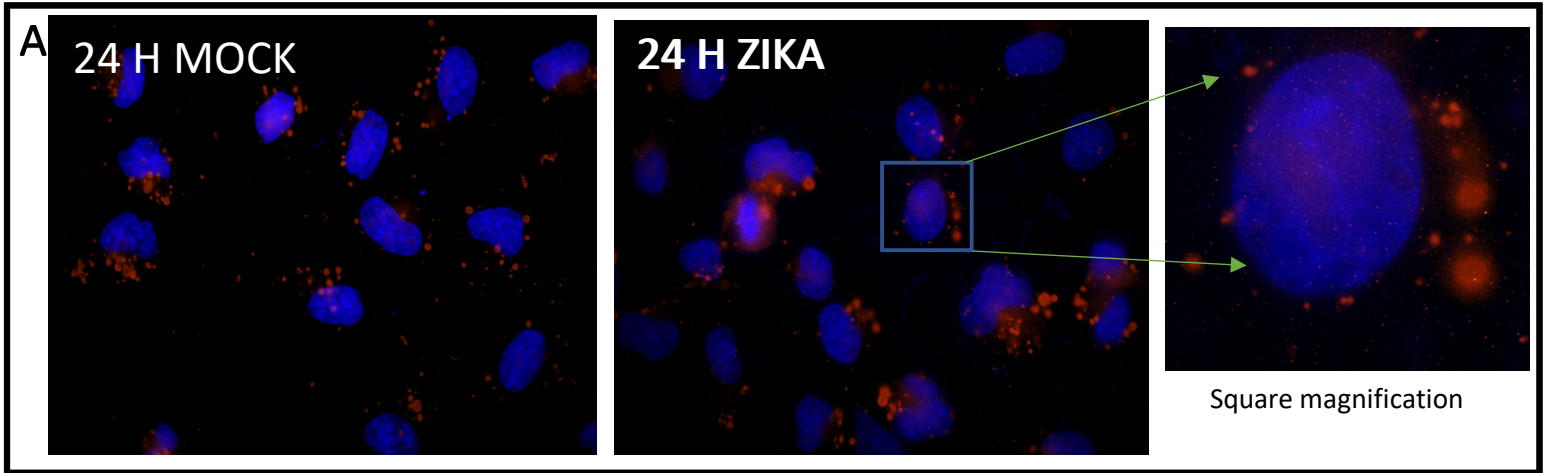


Figure 1: Zika infection changes LD morphology in a time dependent manner. We set out to see if zika infection alter LDs. LDs are stained red (Oil Red O) particles in both mock and zika infected cells after 24 h and 48 h of infection (MOI 1). A. While cells in culture accumulate some LDs even if they are not infected (mock); those infected show an increase in lipid droplets. Right panel show magnified details of a selected cell from the microscopic field (square magnification). B. At 48 H the diameter of the LDs in the zika infected cells is smaller but there are more lipids per cell compared to zika infected cells at 24 H. Right panel show magnified details of a selected cell from the microscopic field. C. Measuring LDs as total red fluorescence per cell, lipid accumulation doubles in infected cells, a significant increase at each time point. D. Production of viral RNA as detected by PCR and is expressed as fold change over mock NS1 expression. There is more viral RNA at 48 H compared to 24 H. Similar fold change values were obtained from three independent experiments. LD quantifications were done by analyzing more than 200 cells for each condition. Images shown here are representative of at least three independent experiments.

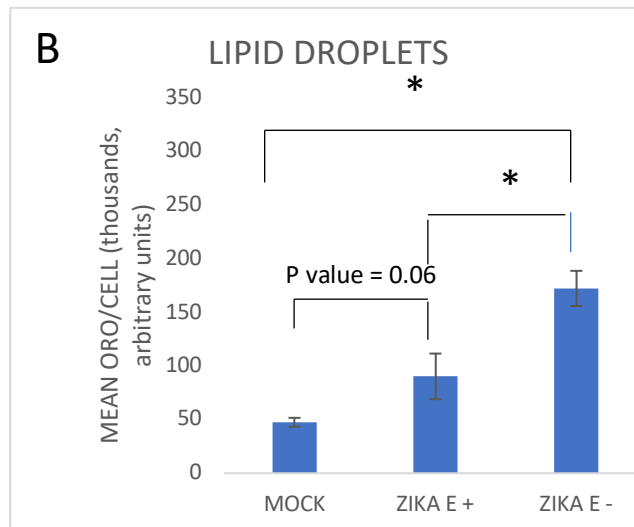
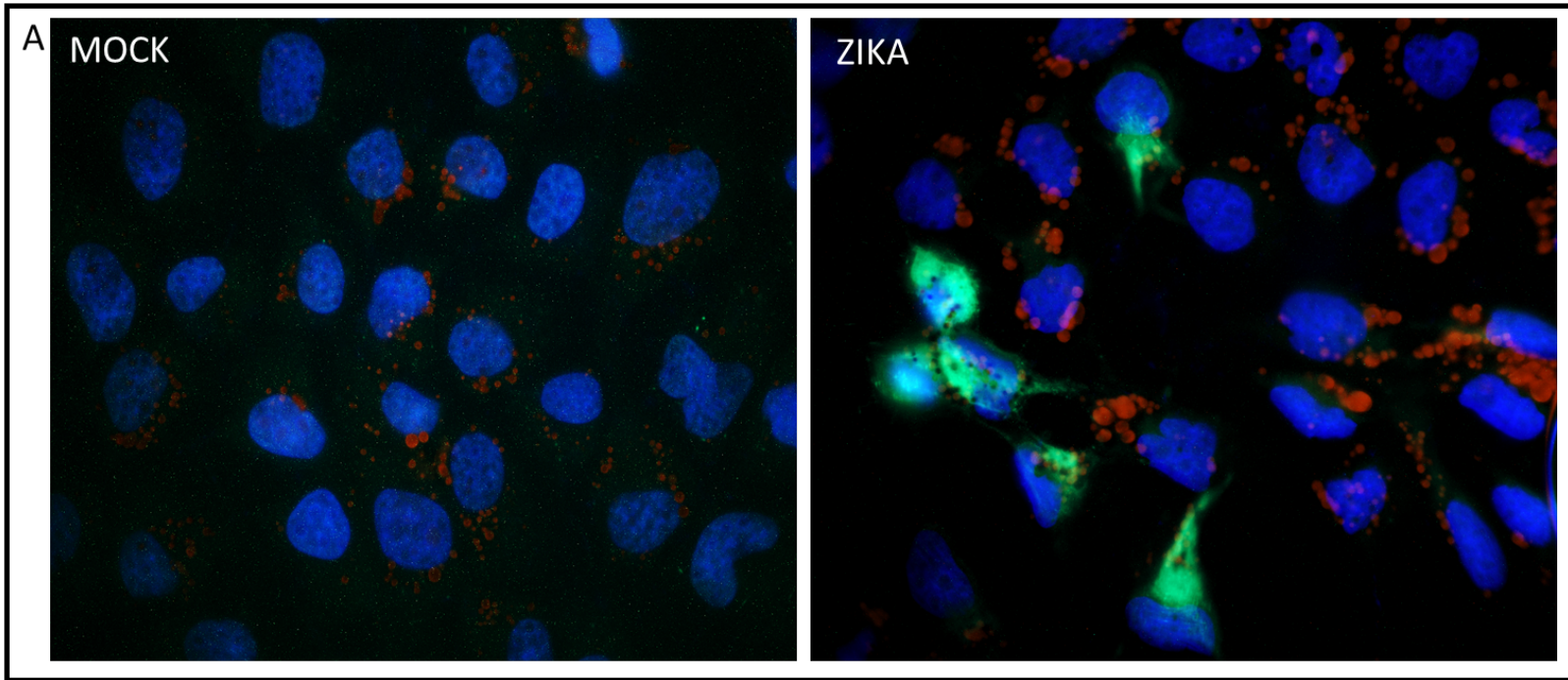


Figure 2: Zika infection modulates lipid droplet in infected and neighboring cells. We next wanted to see the colocalization of lipid droplets in infected cells. Lipid droplets are stained red (Oil Red O) particles in both mock-infected (mock) and infected (zika) cells after 48 h at MOI 1. A. Not all cells were infected, those infected display E protein (green). While the infected cells show variability in the expression lipid droplets, we see that there are more lipid droplets in zika infected cells compared to the neighboring uninfected cells. This is exhibited by ImageJ quantification showing a statistically significant increase when comparing zika infected cells (ZIKV E+) versus uninfected cells in zika condition (ZIKV E-) (2B). The images shown are representative of the condition. Quantification are analyzed in more than 200 cells for each condition.

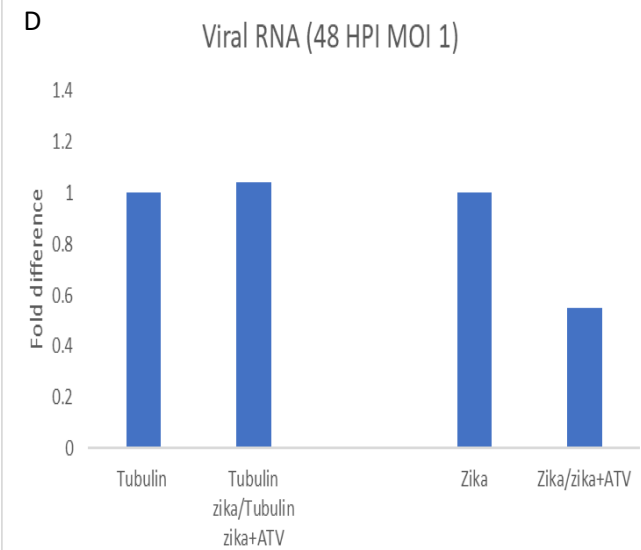
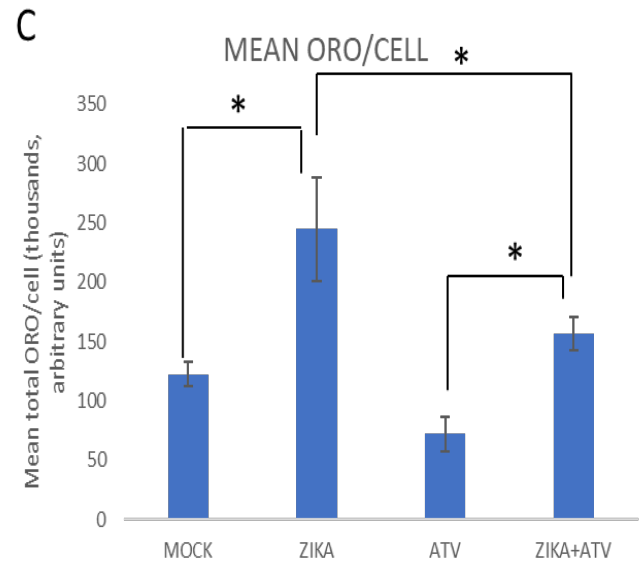
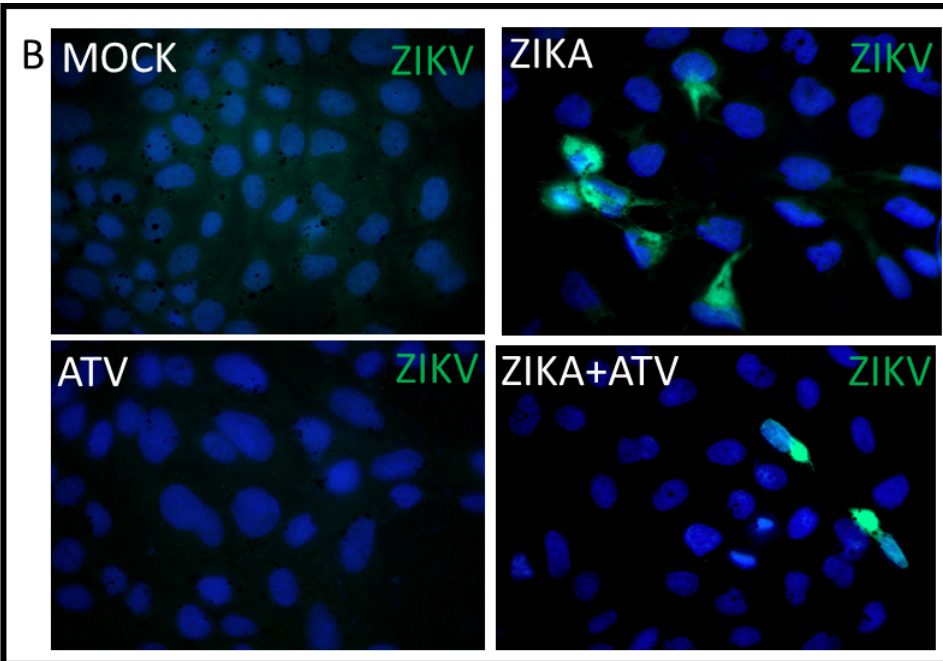
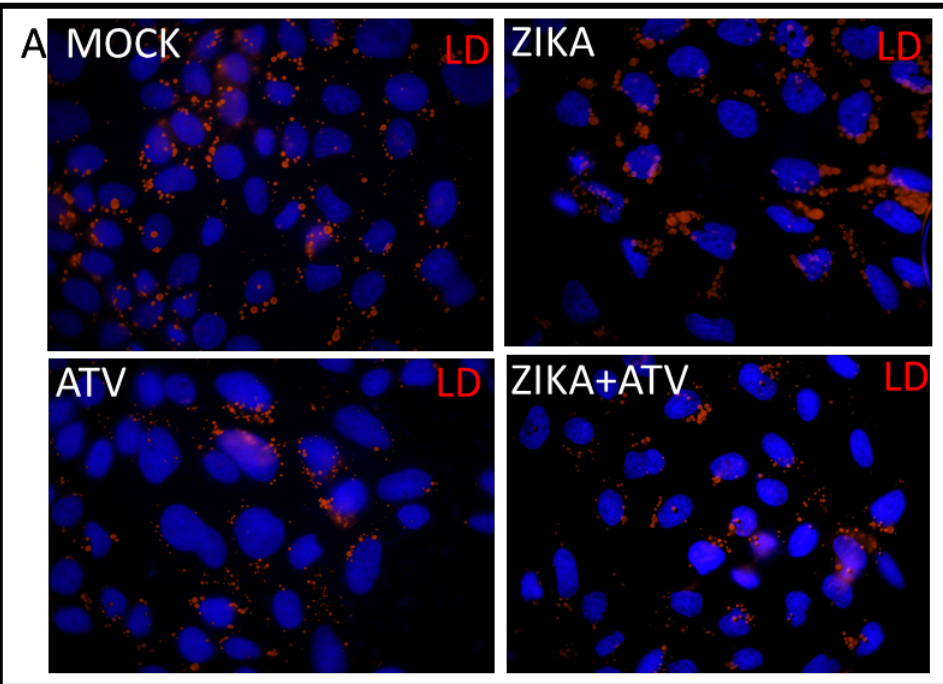


Figure 3: Atorvastatin reduces virus induced lipid droplet formation and inhibits zika virus production. We wanted to see if altering lipid droplets changes zika infection levels. ATV at 5 μ M, applied 1 hour before infection, brings lipid droplet in infected cells (MOI 1) to the level of mock-infected cells (3A, ATV+Zika vs Zika, and this difference is significant (3C, zika vs zika+ATV). ATV treatment partially blocks reproduction of zika by two mechanism: Expression of viral E protein detected by immunofluorescence (Fig. 3B) and production of viral RNA as detected by PCR (Fig. 3D). The images shown are representative of the condition. Quantifications are analyzed in more than 200 cells for each condition.

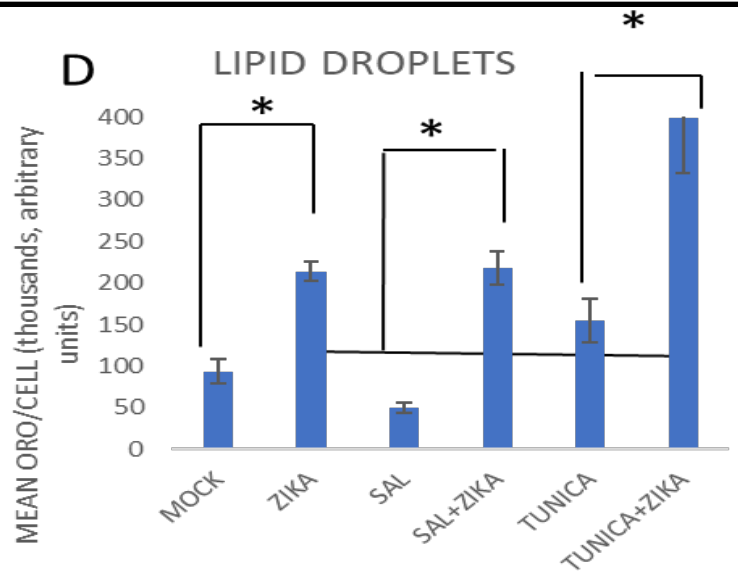
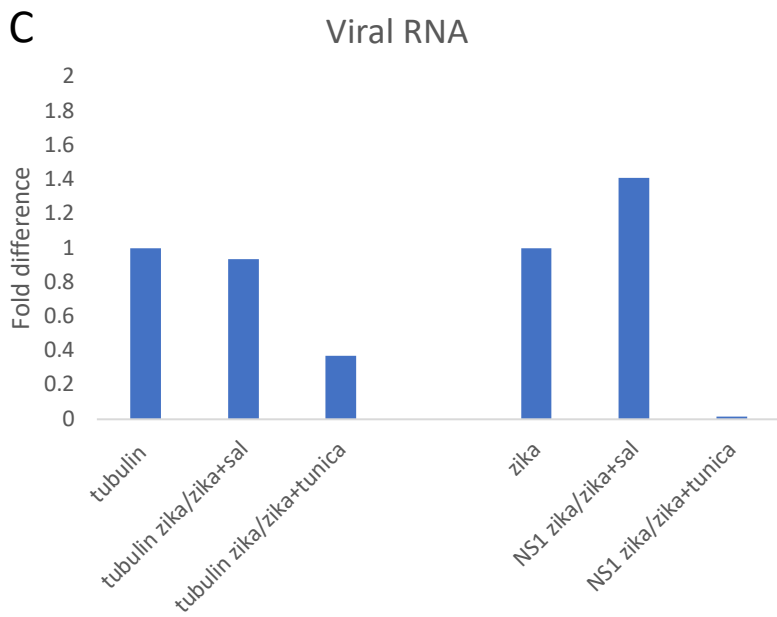
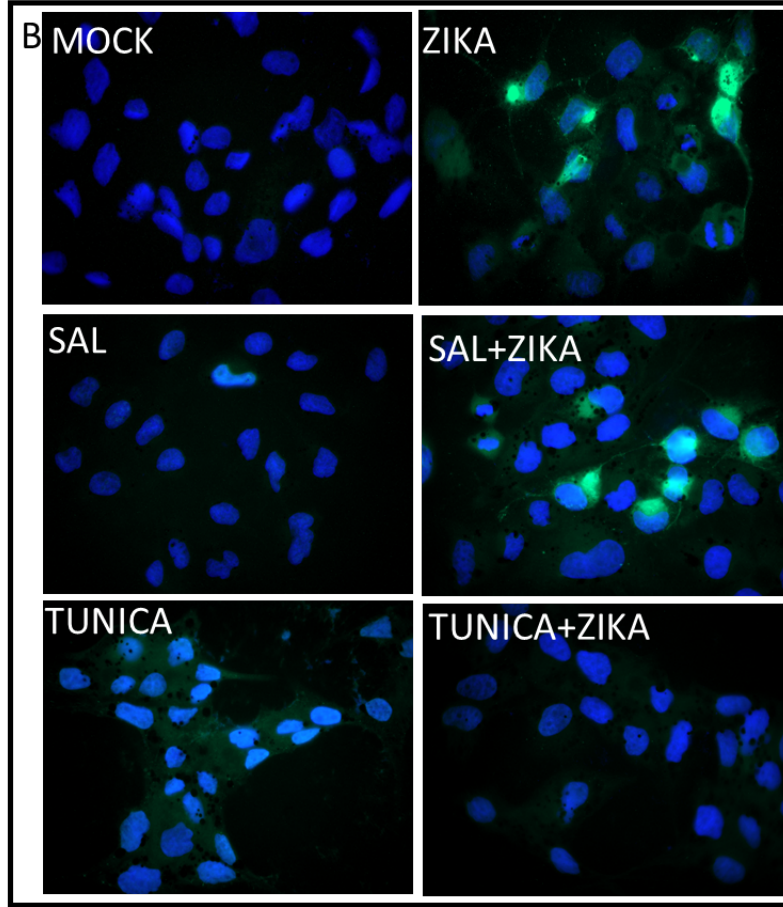
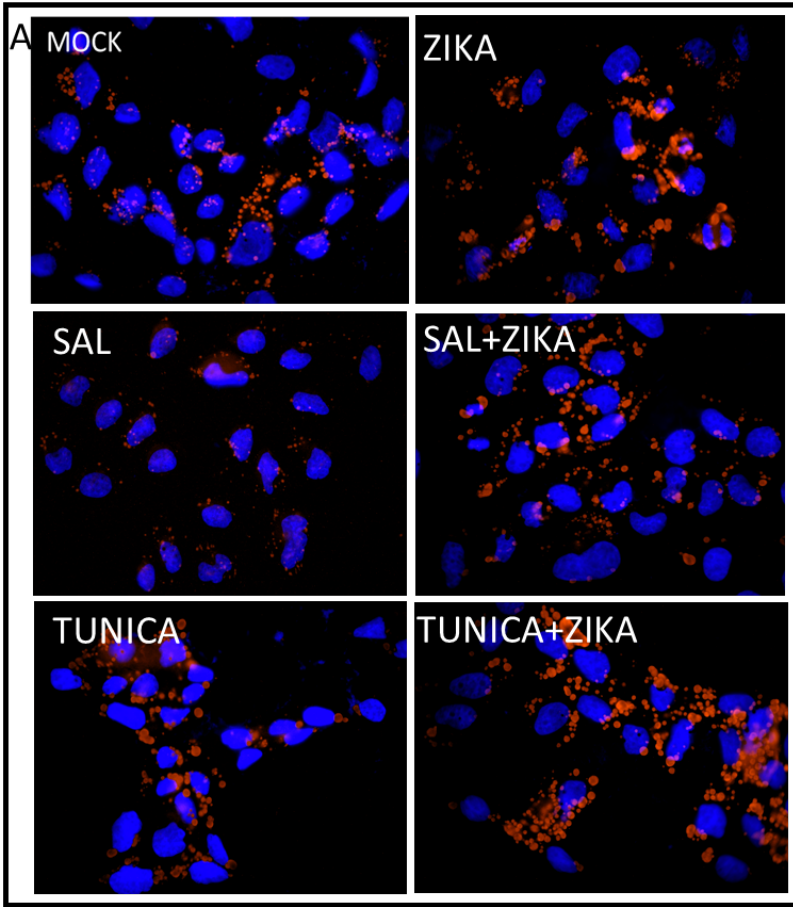


Figure 4. Zika induced lipid droplet accumulation is PERK independent. We hypothesized that lipid droplets may accumulate through the ER stress pathways specifically the PERK pathway. To investigate this, MDCK cells were pretreated either with PERK stress inhibitor, salubrinal (sal) or ER stress inducer, tunicamycin (tunica) at 3uM applied 1 hour before infection. Sal partially though not completely suppresses the formation of lipid droplets (4A compare mock vs sal). However sal has no effect after zika infection (4A compare zika vs sal+zika). Tunica dramatically increases lipid droplet diameter and number (4A compared mock vs tunica). Comparing zika vs tunica+zika we see a dramatic increase in lipid droplets in the tunica treated cells. These observations were corroborated with ImageJ quantification and were statistically significant (4D). Viral E protein was detected by immunofluorescence (4B) and viral RNA was detected by PCR (4C); sal treated zika cells had more viral RNA and E protein expression than whereas the tunica treated infected cells had less viral RNA (4C) and no E protein expression compared to zika alone (4B). The images shown are representative of the condition. Quantifications are analyzed in more than 200 cells for each condition.

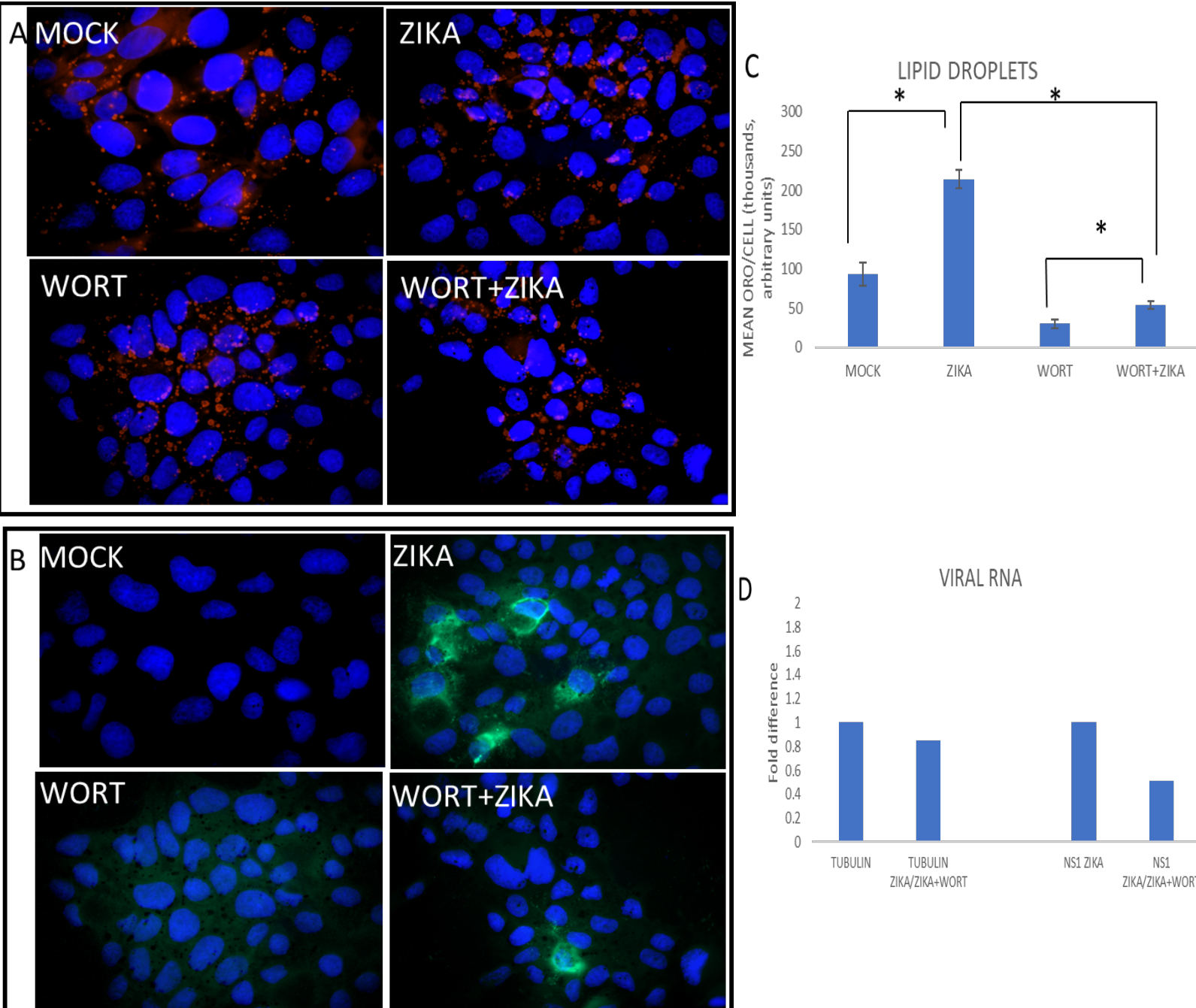


Figure 5: Autophagy inhibition decreases lipid droplets. We questioned whether autophagy triggers lipid accumulation. MDCKs were pretreated with autophagy inhibitor wortmannin at 50 μ M, 1 hour before infection. We find that wortmannin partially blocks the induction of lipid droplets by zika (zika+wort vs zika) (5A). This reduction during autophagy inhibition is significant (5C, compare zika+wort vs wort). Viral replication is decreased in the presence of wortmannin as detected by immunofluorescence (5B) and PCR (5D). The images shown are representative of the condition. Quantifications are analyzed in more than 200 cells for each condition.

